



Trans. Nonferrous Met. Soc. China 24(2014) 1202-1209

Transactions of Nonferrous Metals Society of China

www.tnmsc.cn

Effect of copper, sulfur, arsenic and antimony on silver distribution in phases of lead blast furnace

J. CHAIDEZ-FELIX¹, A. ROMERO-SERRANO¹, A. HERNANDEZ-RAMIREZ¹, M. PEREZ-LABRA², I. ALMAGUER-GUZMAN³, R. BENAVIDES-PEREZ³, M. FLORES-FAVELA³

- 1. Metallurgy and Materials Department, IPN-ESIQIE, UPALM, Zacatenco, C.P. 07738, Mexico D.F., Mexico;
 - 2. Academic Area of Earth Science and Materials, UAEH, Col. Carboneras,

Mineral de la Reforma, C.P. 42184, Hidalgo, México;

3. Servicios Administrativos Peñoles S.A de C.V. Prol. Comonfort Sur 2050, Col. L. Echeverria, Torreon, C.P. 27300 Coahuila, Mexico

Received 9 August 2013; accepted 17 November 2013

Abstract: An experimental study was carried out to estimate the effect of the lead impurities on the silver distribution in the phases formed in the lead blast furnace. Samples of sinter with different contents of Cu, S, As and Sb were equilibrated under reducing atmosphere $(p(CO)/p(CO_2)=2.45)$ at 1573 K in a tube furnace and slowly cooled. The samples were characterized by scanning electron microscopy and microanalysis (SEM-EDS). There were five immiscible phases: slag (CaO, FeO and SiO₂), matte (S, Cu and Fe), speiss (As, Fe and Cu), Cu–Sb phase and lead bullion (Pb, Ag, Sb, Cu, etc). The results showed that Cu and Sb promote silver losses during the process since they form a liquid solution with higher silver solubility than liquid bullion. Sulfur and arsenic react with copper to form the matte and speiss phases, respectively. The effect of S and As is to reduce the amount of Cu–Sb alloy and then the silver losses from the bullion.

Key words: lead blast furnace; silver; lead impurities

1 Introduction

The main source of lead is galena, PbS, which is concentrated by flotation, containing metallic impurities such as iron, copper, zinc, arsenic, antimony, tin and precious metals. The oxidation roasting of lead sulfide concentrates and the partial melting of these materials are used to remove sulfur from the condensed phases, and to agglomerate the fine particles into porous oxide materials that are used as feedstock for the lead blast furnace [1]. Blast furnace is still the predominant technology used to produce primary lead metal. Sinter, coke and CaO are fed to the lead blast furnace; the coke reacts with oxygen at high temperatures and produces a reducing atmosphere inside the furnace, giving CO as main reducing gas.

A calculated amount of CaO ensures to get low viscosity in the lead slag [2] and a low operation temperature at the bottom of the furnace [3]. The lead blast furnace is a reactor where the charge moves

through a vertical shaft in countercurrent to the ascending reducing gas flow. The descending charge successively passes through the preheating zone (473 K), the reaction or reduction zone (1173 K), the melting zone (1423 K), and finally the combustion zone (tuyere zone). The produced liquid phases (slag, matte, speiss and bullion) are collected in the furnace crucible [4,5], and separated by density gradient.

The sinter produced in Mexico has historically been different from that around the world in which the Mexican sinter contains high silver and bismuth concentrations.

CHAO et al [6] and MORRIS et al [7] reported the gas composition, temperature and pressure as a function of the height above the tuyeres in a commercial lead blast furnace. It was shown that at the tuyere level the temperature was between 1473 K and 1573 K and the CO-to-CO₂ volume ratio was between 2 and 2.5. PEREZ-LABRA et al [8] reported that lead oxide is easily reduced under the atmosphere with $p(\text{CO})/p(\text{CO}_2)$ =2.45 at the temperature at the tuyere level.

The recovery of precious metals during lead production in a blast furnace makes this process more profitable. However, very few experimental reports are available to describe the behavior of silver under the industrial process conditions. Losses of silver and lead are common in this process due to both physical and chemical phenomena. Lead can be trapped as metallic particles in the slag [9], due to its composition and viscosity. CALVO and BALLESTER [10] reported the effect of the oxygen potential on the lead trapped in the slag; the results showed that an appropriate oxygen potential keeps the slag with very low content of lead. KHATIBI [11] reported the effect of the CaO content on the distribution of elements in slag, matte and speiss in the copper process. In the present work, the effect of the impurities (Cu, S, As, and Sb) on the distribution of silver in the phases produced at high temperature (1573 K) is analyzed.

2 Experimental

The experimental design was based on the sinter compositions used in typical industrial lead blast furnaces. Several sinter samples were selected to study one of the following composition parameters Cu, S, As and Sb contents, keeping the composition of the other components constant as far as possible. Tables 1–4 show the sinter compositions to test the effect of copper, sulfur, antimony and arsenic, respectively. Silver contents in all the samples were between 4500 and 5500 g/t.

Table 1 Sinter compositions to evaluate effect of copper

Sample No.	w(S)/%	w(Cu)/%	w(As)/%	w(Sb)/%
1	1.95	2.04	0.476	0.447
2	1.95	2.56	0.504	0.506

Table 2 Sinter compositions to evaluate effect of sulfur

Sample No.	w(S)/%	w(Cu)/%	w(As)/%	w(Sb)/%
3	1.52	2.02	0.480	0.378
4	2.23	2.06	0.476	0.390

Table 3 Sinter compositions to evaluate effect of antimony

Sample No.	w(S)/%	w(Cu)/%	w(As)/%	w(Sb)/%
5	1.85	2.12	0.546	0.328
6	1.87	2.20	0.580	0.484

Table 4 Sinter compositions to evaluate effect of arsenic

Sample No.	w(S)/%	w(Cu)/%	w(As)/%	w(Sb)/%
7	2.10	2.41	0.406	0.431
8	1.87	2.20	0.580	0.484

25 g of each sinter sample was crushed into fine powders, homogenized and equilibrated for 4 h in a stainless steel crucible at 1573 K (1300 °C). These experiments were carried out in a tubular resistance furnace. The atmosphere within the reaction tube was kept at a fixed oxygen partial pressure $(p(O_2)=1.2765 \mu Pa$ at 1573 K) using a flow of 150 mL/min with $p(CO)/p(CO_2)=2.45$. The furnace temperature was controlled within ± 3 K with an R-type thermocouple (Pt-Pt, 13%Rh).

After the equilibrium was reached, the furnace was turned off and the samples were slowly cooled, allowing the phases to be separated by their density gradient. Then, the samples were cut along the longitudinal axis of the crucible. The microstructural analysis was performed by first mounting and polishing the samples, then by examination using both optical microscopy (OM) and scanning electron microscopy (SEM) coupled with an energy-dispersive spectra (EDS) analyzer. Measurements of the compositions of the phases were undertaken using a SEM-Jeol 6300 electron probe microanalyzer (PMA) with wavelength dispersive detectors.

A thermodynamic analysis was carried out using the software FACTSage 6.4 (facility for the analysis of chemical thermodynamics) [12] in order to estimate the effect of the sinter composition on the phases formed at high temperature and under a reducing atmosphere. An analysis of the ternary phase diagrams was also included to explain the chemical affinity among Pb, Cu, Sb and Ag.

3 Results and discussion

3.1 Effect of copper

Figure 1 shows the microstructure of typical sinter equilibrated a 1573 K. The phase assemblages shown in Fig. 1(a) corresponds to the image along the longitudinal axis of the system, where the crucible is at the bottom, then there is the bullion followed by a zone of interfaces (Cu–Sb alloy, speiss and matte) and at the top there is the slag. Figure 1(b) shows a magnification of the interface zone. The slag phase appears in this figure as dark globules and the lead bullion as a light zone. Figure 1(c) shows Cu–Sb dendritic precipitates in the bulk of the bullion phase.

Figure 2 illustrates the microstructure obtained at the interface zone on a sinter with high copper content (2.56%Cu). The compositions of the phases were measured with EDS and are presented in Table 5. Each phase composition given in this figure is an average of up to five compositions measured in various locations within that phase. The slag mainly contains oxygen, silicon, calcium and iron; then, probably they are calcium and iron silicates. The speiss phase is formed

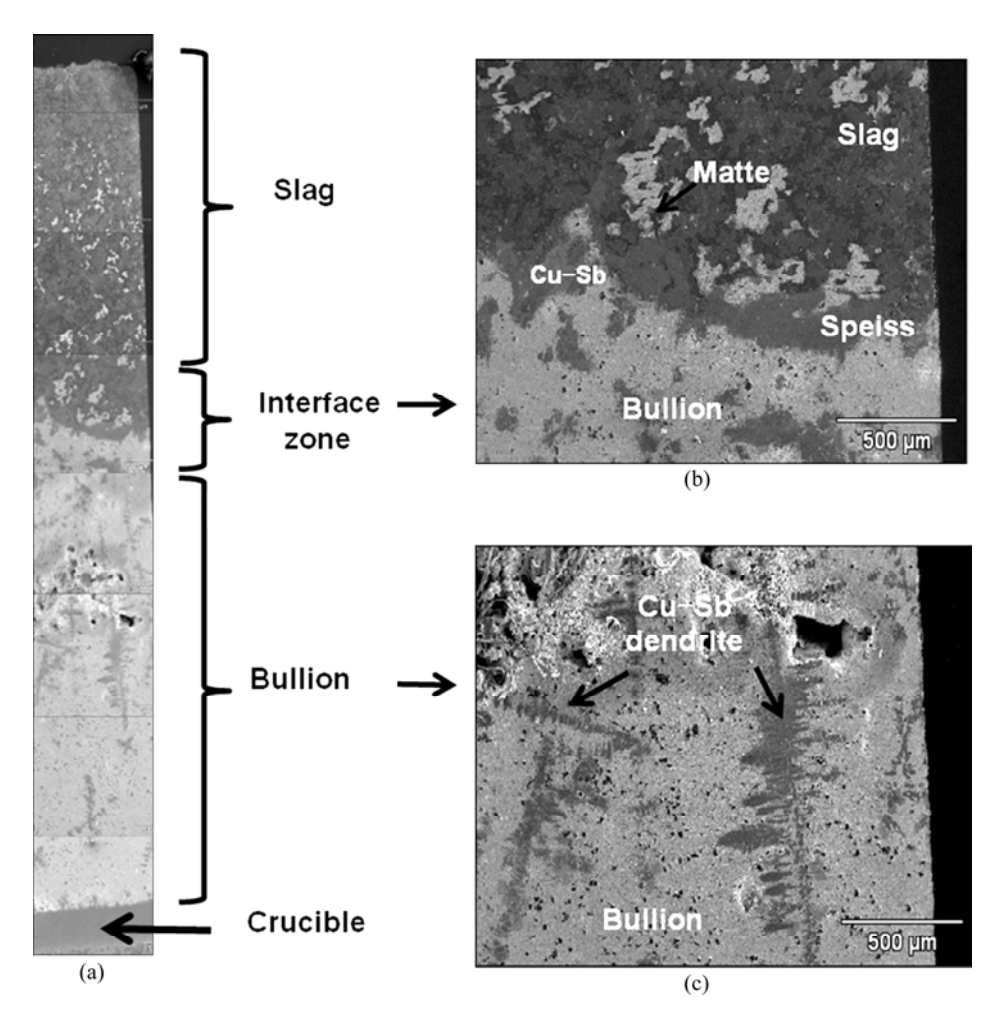


Fig. 1 SEM images showing phase assemblages of phases equilibrated at 1573 K

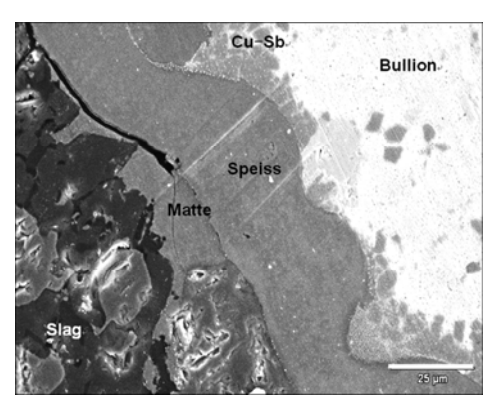


Fig. 2 SEM image showing microstructure obtained at interface zone on Sample No. 2 with high copper content (2.56% Cu)

by iron, arsenic and small amount of copper, whereas the matte phase has sulfur, copper and iron. It is worth to note that silver is mainly in the bullion phase but it is also found in the Cu-Sb particles.

The microstructure and X-ray mapping images for Ag, Cu, Sb, S and Pb elements in the interface zone of Sample No. 2 with high copper content (2.56% Cu) is given in Fig. 3. The X-ray mappings show a contrast due

to element concentration gradient. For example, in the X-ray image for silver, the bright areas correspond to silver-rich zones and the dark areas correspond to silver-poor zones. This figure shows that copper is associated with sulfur in the matte phase and with Sb in the Cu–Sb phase. The X-ray mappings also show that silver is close to the Cu–Sb phase but it is neither contained in the slag nor in the matte phases.

The Cu-Sb phase was not only observed in the interface zone, between the speiss and the bullion, but also in the bulk of the bullion as dendritic precipitates. Figure 4 shows an example of the microstructure of these dendrites together with the X-ray mapping images for the Ag, Cu and Sb elements for Sample No. 2. It is again observed that there are silver particles near the Cu-Sb phase.

Figures 5 and 6 show the ternary phase diagrams for the Ag-Cu-Pb and Sb-Cu-Pb systems [13], respectively. It is observed that in both systems there is a miscibility gap, where two liquids are immiscible, one is a Cu-rich liquid phase and the other is a Pb-rich liquid phase. The compositions of the two liquids are given by the

Table 5 Chemical composition of phases obtained in interface zone on Sample No. 2 with high copper content (2.56% Cu)

Phase	w(O)/%	w(Si)/%	w(S)/%	w(Ca)/%	w(Fe)/%	w(Cu)/%	w(As)/%	w(Ag)/%	w(Sb)/%	w(Pb)/%
Bullion	4.00	0.17	0	0.09	0.13	1.08	0	3.99	1.26	89.28
Cu-Sb	1.63	0.08	0	0	0.60	63.23	1.15	0.77	27.46	5.08
Speiss	0	0.17	0	0.05	90.94	1.86	6.93	0	0.05	0
Matte	2.30	0	26.54	0.04	14.14	55.22	0	0	0	1.76
Slag	28.66	16.78	0	27.24	23.18	0.24	0	0	2.51	1.39

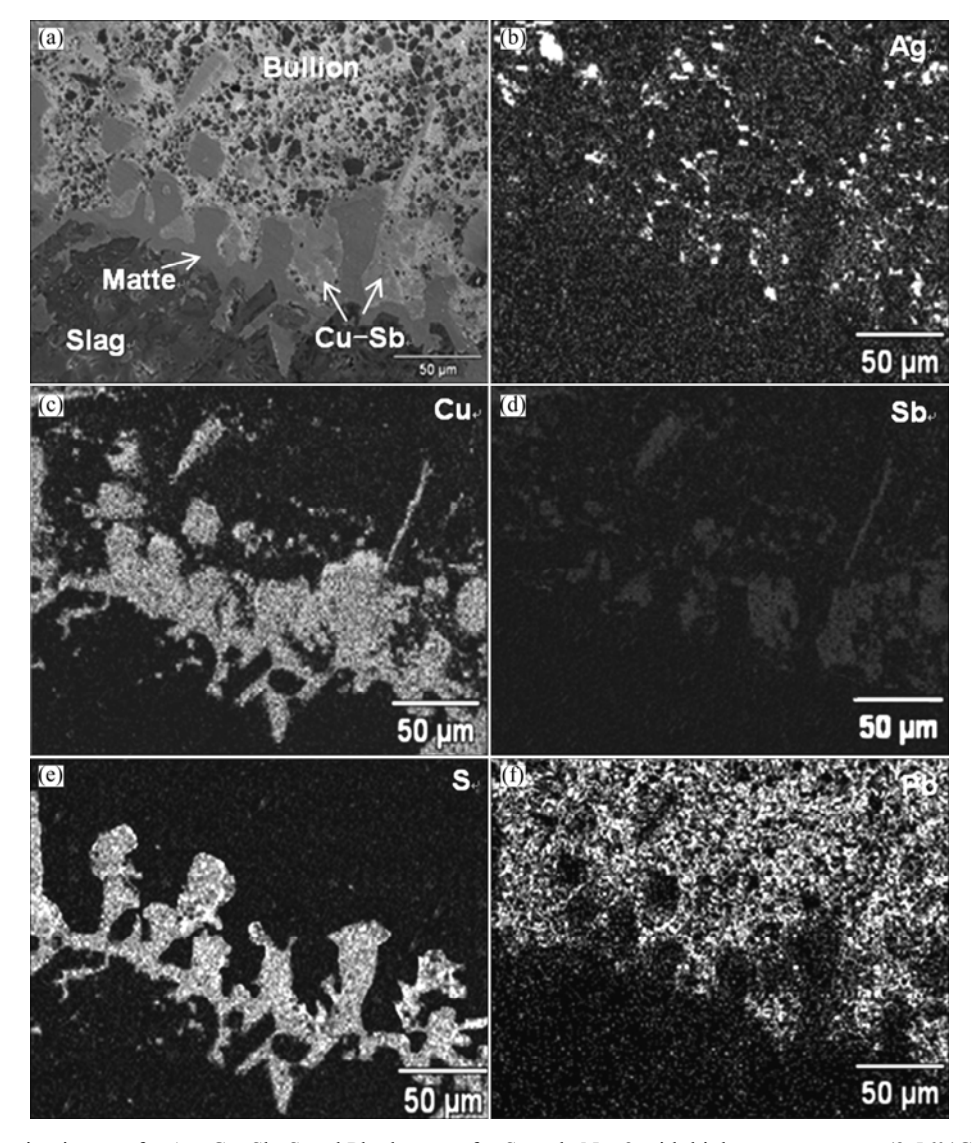


Fig. 3 X-ray mapping images for Ag, Cu, Sb, S and Pb elements for Sample No. 2 with high copper content (2.56%Cu)

intersection of the tie line with the boundary of the twoliquid region. The tie lines of both ternary phase diagrams show that the Cu-rich liquid may dissolve an amount of silver (or antimony) higher than the Pb-rich liquid.

The ternary phase diagrams of Ag-Cu-Pb and Sb-Cu-Pb explain the high silver concentration close to the Cu-Sb phase, shown in Figs. 3 and 4. The higher silver solubility in the Cu liquid phase diminishes the silver content in the near lead liquid. However, as the system is cooled down, the Ag solubility in the Cu-Sb phase is

diminished and it precipitates as almost pure silver. Since the system is cooling down, there is not enough time for the Pb liquid to reabsorb completely the silver particles.

In an industrial process, slag is separated from the bullion at the same time that the liquid products are leaving the lead blast furnace. If the slag viscosity is high and the settling time is not enough to separate efficiently the phases, the slag product can take part of the adjacent phases; hence, the presence of the Cu–Sb phase trapped in the slag will increase the silver loss in the slag.

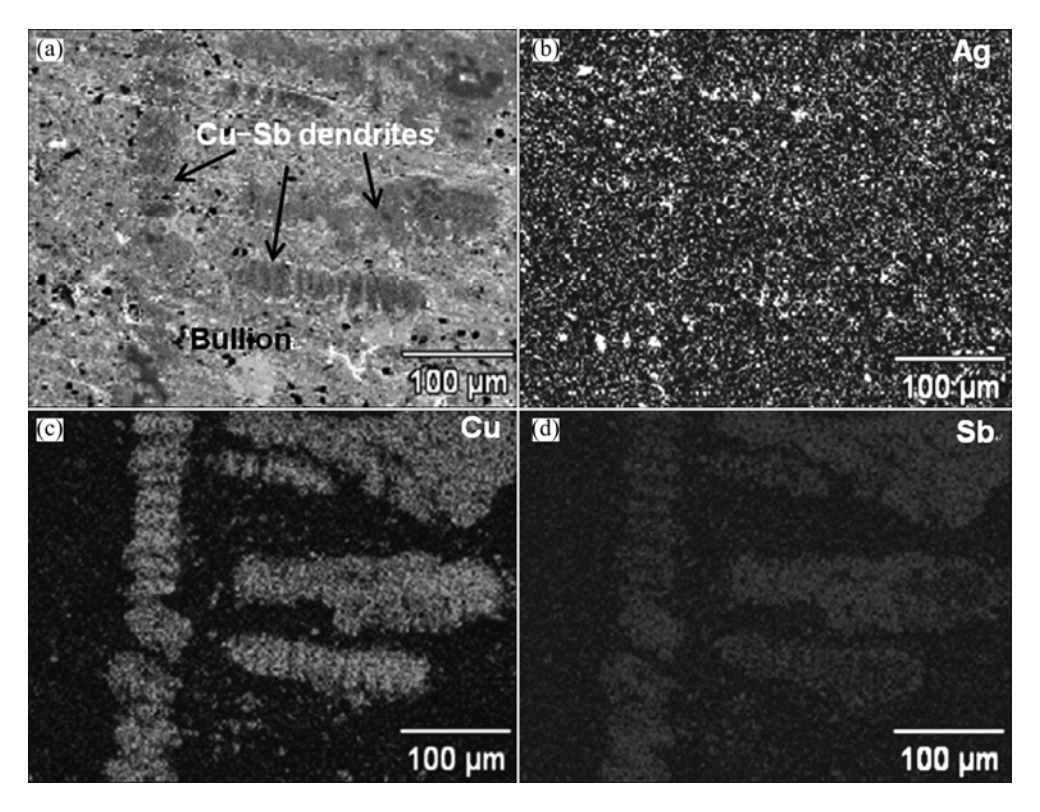


Fig. 4 Dendrites of Cu-Sb present in bulk of bullion and X-ray mapping images for Ag, Cu and Sb elements

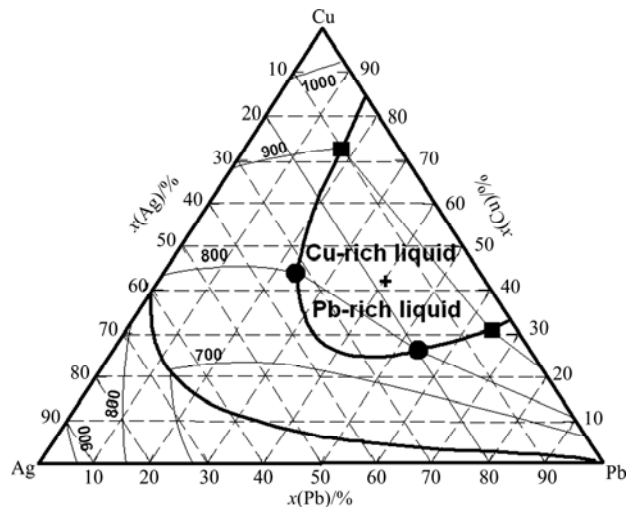


Fig. 5 Ternary phase diagram of Ag-Cu-Pb system [13]

3.2 Effect of sulfur

In order to elucidate the effect of sulfur on the silver loss in the lead blast furnace, two sinter samples were investigated, a low-sulfur sinter (1.52% sulfur in mass fraction) and a high-sulfur sinter (2.23% sulfur in mass fraction), as shown in Table 2. Figure 7 shows the microstructure and the X-ray mapping images for the Sb, Cu and S elements in the interface zone of Sample No. 4 with high sulfur content. As shown in this figure there is a considerable amount of matte phase in the system, where copper and sulfur are associated, much higher than the amount of the Cu–Sb phase. Thus the majority of the

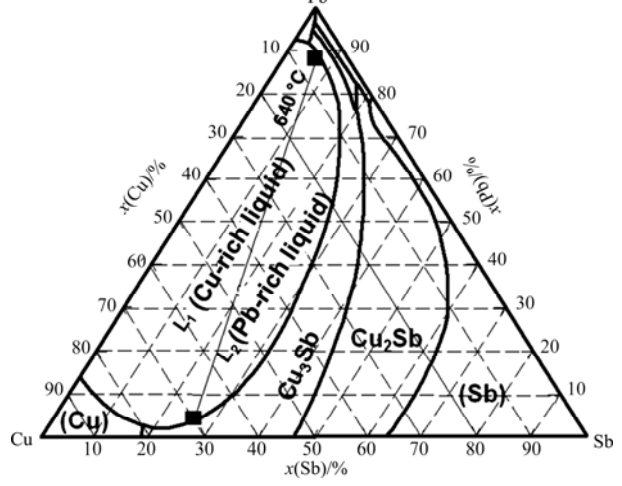


Fig. 6 Ternary phase diagram of Sb-Cu-Pb system [13]

copper remains dissolved in the matte. Since silver is found only in the bullion and in the Cu–Sb phase, an increasing sulfur content in the system results in higher copper content in the matte, resulting in lower silver losses to the Cu–Sb phase.

To support the experimental results of the effect of sulfur on the silver losses, the experimental conditions were modeled using the Equilib module of FactSage 6.4 [12]. The Equilib module is meant for the calculation of so-called complex equilibria, i.e., equilibrium states of multi-component multi-phase systems comprising many non-ideal condensed solutions. This software was used to

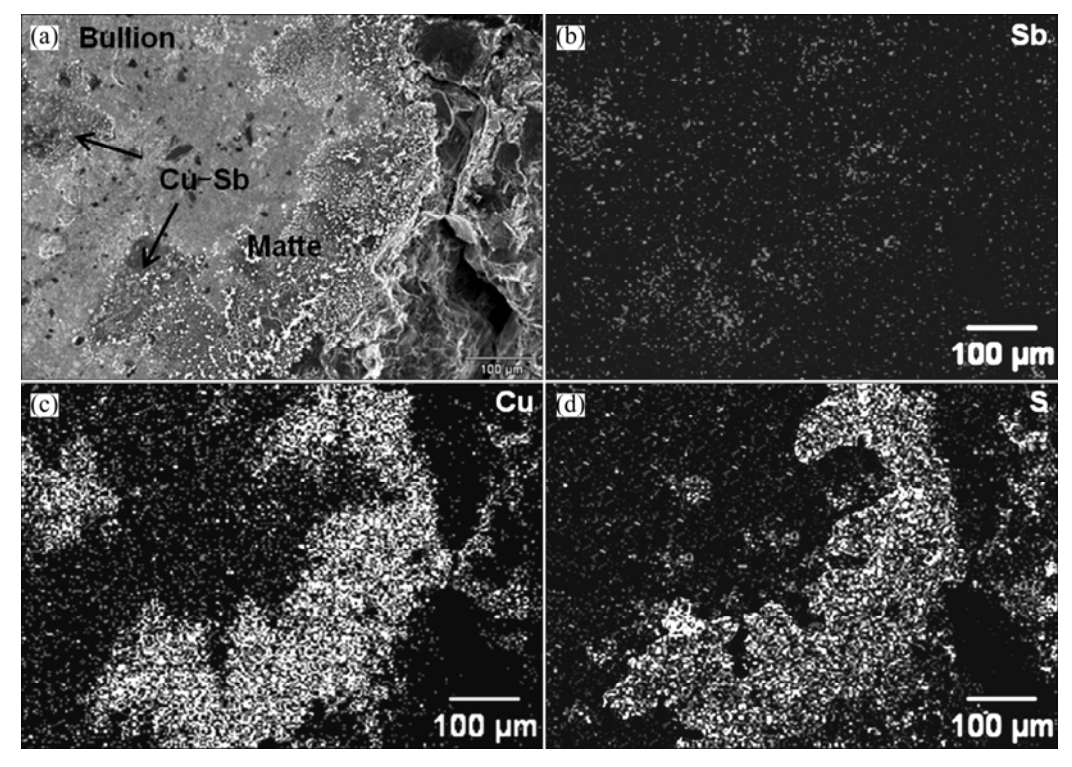


Fig. 7 X-ray mapping images for Sb, Cu and S elements for Sample No. 4 with high sulfur content

calculate the thermodynamic changes in the copper contents of the matte and the Cu-Sb phases as a function of the sulfur content in the system. FactSage uses a modified quasi-chemical model for the molten slag phase. The other phases considered in this calculation were the liquid matte phase, Cu liquid alloy, speiss (Fe-As) and lead liquid alloy.

We consider in the calculations a typical sinter composition given in Table 6, at 1573 K under a reducing atmosphere of $p(\text{CO})/p(\text{CO}_2)=2.45$ ($p(\text{O}_2)=1.2765~\mu\text{Pa}$ at 1573 K). The sulfur content was simulated by assuming that the sinter has different amounts of lead sulfide. Figure 8 shows the effect of PbS content on the copper distribution between the matte and the Cu–Sb liquid phase. In general, higher sulfur content in the system can increase the matte and diminish the Cu–Sb phase, therefore reducing the silver losses to this phase.

Table 6 Sinter composition to calculate effect of sulfur on copper distribution between matte and Cu–Sb phases

Species	Content/g	Species	Content/g
$Pb_{3}Ca_{2}Si_{3}O_{11} \\$	32.0	CuFe ₂ O ₄	3.13
$ZnFe_2O_4$	28.54	Pb ₂ Fe ₂ Si ₂ O ₉	2.92
PbO	9.36	CaSO ₄	2.02
$PbSO_4$	6.76	ZnO	1.93
$Ca_2ZnSi_2O_7$	5.08	Zn ₂ SiO ₄	1.05
CuO	3.58	SiO ₂	0.27
Ca ₃ Si ₂ O ₇	3.36		

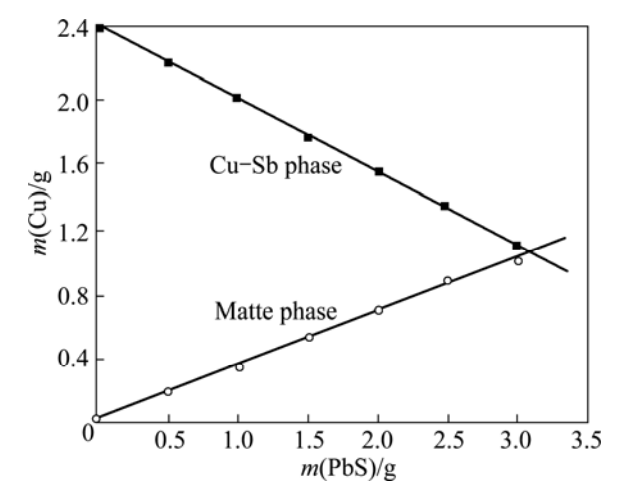


Fig. 8 Effect of sulfur content in sinter on copper distribution in matte and Cu-Sb phases

3.3 Effect of antimony

The thermo-chemical standard software FactSage was also used to estimate the effect of the antimony on the silver solubility in the Cu–Sb liquid alloy at 1298 K and 1323 K. Figure 9 shows that at a given temperature, the silver solubility in the molten Cu–Sb phase increases with the increase of antimony content. It is also observed that the silver solubility is increased with temperature as it was expected.

3.4 Effect of arsenic

Some lead mineral resources have relatively high

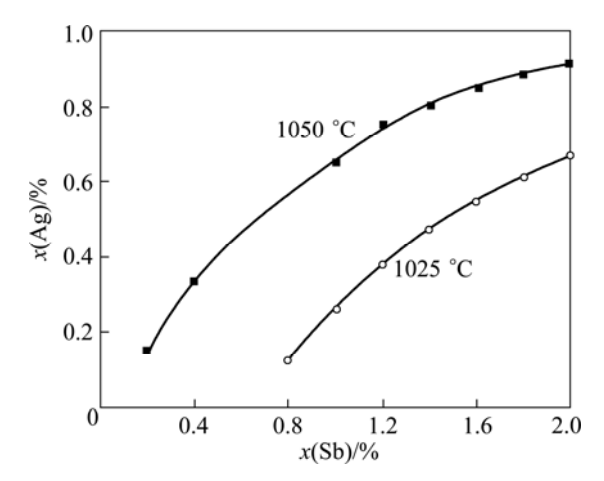


Fig. 9 Effect of antimony content on silver solubility in Cu-Sb-Ag liquid phase

content of arsenic, thus it is important to estimate the effect of this element on the silver distribution in the phases formed in the lead blast furnace. Arsenic and iron form the speiss phase; however, when the arsenic content in the system is high, copper can also be incorporated into this phase. The affinity of copper for arsenic is higher than the affinity for antimony. This is concluded from the negative values of the standard Gibbs free energy of reaction (1) at any temperature.

$$3Cu_2Sb + 2As \rightarrow 2Cu_3As + 3Sb$$
 (1)

The microstructural evidence of the formation of a Cu-Fe-As speiss phase is shown in Fig. 10. This figure corresponds to Sample No. 8 whose composition is shown in Table 4. The compositions of the phases measured with EDS are also presented in Table 7. There are two speiss phases. One contains Fe and As and a low amount of copper (1.53%Cu), the other speiss phase contains 12.78% Cu. It is also observed that the amount of the Cu-Sb is low and most of copper is in the Fe-Cu-As speiss.

The experimental results show that arsenic and sulfur react with copper and reduce the amount of the Cu–Sb phase; then, these elements may improve the silver recovery in the bullion phase.

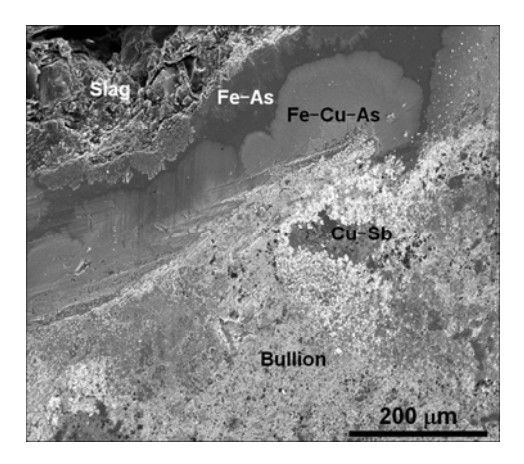


Fig. 10 Microstructure of phases obtained on Sample No. 8 with high arsenic content (0.58 % As)

4 Conclusions

- 1) The phases formed are: bullion, Cu–Sb, speiss, matte and slag. The Cu–Sb phase was obtained between the bullion and speiss, as well as in the bulk of the bullion phase with a dendritic growth. In all the samples there was a high concentration of Ag close to the Cu–Sb phase.
- 2) Copper is a silver collector, thus it can promote the silver initially inside the bullion to be dragged to the interface zone, close to the speiss and matte phases. Antimony contained in the sinter enhances the formation of the Cu–Sb phase and increases the silver solubility in this phase.
- 3) Arsenic forms a speiss phase with iron, but when the content of arsenic increases, copper will be also dissolved in this phase. On this way, arsenic can decrease the formation of the Cu–Sb phase, and accordingly the solubility of silver in the Cu–Sb liquid will decrease. Sulfur can also decrease the formation of the Cu–Sb phase due to the formation of matter phase.

Acknowledgements

The authors thank Servicios Administrativos Peñoles S.A. de C.V. for providing financial support for this project. The authors wish also to thank the

Tabel 7 Chemical composition of phases obtained on Sample No. 8 with high arsenic content (0.58% As)

Phase	w(O)/%	w(Si)/%	w(Ca)/%	w(Fe)/%	w(Cu)/%	w(As)/%	w(Sb)/%	w(Ag)/%	w(Pb)/%
Slag	28.4	11.0	43.0	9.20	0.49	0	0	0	7.91
Fe-As speiss	0	0.29	0.01	93.3	1.53	4.87	0	0	0
Fe-Cu-As speiss	2.0	1.62	0.04	78.92	12.78	4.51	0.13	0	0
Cu-Sb	6.29	0.62	0	4.75	32.09	1.80	11.17	0.48	42.80
Bullion	3.07	2.35	0.49	1.08	5.07	0	2.36	0.88	84.70

Institutions CONACyT, COFAA and IPN for their permanent assistance to the Process Metallurgy Group at ESIQIE-Department of Metallurgical Eng.

References

- [1] ZHAO B, ERRINGTON B, JAK E, HAYES P. Gaseous reduction of isasmelt lead slag and lead blast furnace [C]//Lead and Zinc 2008. Johannesburg: The Southern African Institute of Mining and Metallurgy, 2008: 133–146.
- [2] KING M, RAMACHANDRAN V, PRENGAMAN R D, DEVITO S C. Lead and lead alloys [M]. New York: Kirk-Othmer Encyclopedia of Chemical Technology, 2005: 60.
- [3] CALEY W F, WHITEWAY S G, NEIL A B, DUG-DALE P J. Viscometer for lead blast furnace slags [C]//14th Annual Conference of Metallurgists. Toronto: Canada Institute of Metallurgy, 1975: 113.
- [4] HABASHI F. Handbook of extractive metallurgy. Primary metals, secondary metals, light metals [M]. New York: Wiley-VCH, 1997: 2379
- [5] TAN Peng-fu. Thermodynamic modeling of lead blast furrnace [J]. Transactions of Nonferrous Metals Society of China, 2005, 15(1): 160–165.
- [6] CHAO J T, DUGDALE P J, MORRIS D R, STEWARD F R. Gas

- composition, temperature and pressure measurements in lead blast furnace [J]. Metall Trans B, 1978, 9: 293–300.
- [7] MORRIS D R, AMERO B R, EVANS P G, PETRUK W, OWENS D R. Reactions of sinter in a lead blast furnace [J]. Metall Trans B, 1983, 14: 617–623.
- [8] PEREZ-LABRA M, ROMERO-SERRANO A, HERNANDEZ-RAMIREZ A, ALMAGUER-GUZMAN I, BENAVIDES-PEREZ R. Distribution of lead and silver under lead blast furnace conditions [J]. Revista de Metalurgia de Madrid, 2012, 48(3): 213–222.
- [9] CALVO F A, BALLESTER A. Lead ore reduction: Metal losses in the slag [J]. Quimica e Industria, 1984, 30(9): 557–562.
- [10] CALVO F A, BALLESTER A. Lead losses in the slag of a reduction melting furnace. Effect of the slag composition [J]. Anales de Quimica, 1987, 83: 397–406.
- [11] KHATIBI A. Distribution of elements in slag, matte and speiss during settling operation [D]. Lulea: Lulea University of Technology, 2008
- [12] THOMPSON W T, BALE C W, PELTON A D. Facility for the analysis of chemical thermodynamics (FACTSage) [EB/OL]. [2012] Ecole Polytechnique, Montreal. http://www.crct.polymtl.ca
- [13] VILLARS Pierre, PRINCE Alan, OKAMOTO Hiroaki. Handbook of ternary alloy phase diagrams [M]. Ohio, USA: ASM International, 1995.

铅鼓风炉中铜、硫、砷和锑对银分布的影响

J. CHAIDEZ-FELIX¹, A. ROMERO-SERRANO¹, A. HERNANDEZ-RAMIREZ¹,
M. PEREZ-LABRA², I. ALMAGUER-GUZMAN³, R. BENAVIDES-PEREZ³, M. FLORES-FAVELA³

- 1. Metallurgy and Materials Department, IPN-ESIQIE, UPALM, Zacatenco, C.P. 07738, Mexico D.F.;
 - 2. Academic Area of Earth Science and Materials, UAEH, Col. Carboneras, Mineral de la Reforma, C.P. 42184, Hidalgo, México;
 - Servicios Administrativos Peñoles S.A de C.V. Prol. Comonfort Sur 2050,
 Col. L. Echeverria, Torreon, C.P. 27300 Coahuila, Mexico

摘 要: 研究铅鼓风炉中杂质对银分布的影响。将含有不同 Cu、S、As 和 Sb 含量的铅烧结块在管式炉中于 1573 K 下进行烧结,然后随炉冷却。烧结气氛为还原性的 $CO+CO_2$ 气体($p(CO)/p(CO_2)=2.45$)。采用 SEM-EDS 对所得样品进行表征。结果表明:烧结样品中含有 5 种不互溶的相,即炉渣(CaO, FeO, SiO $_2$)、冰铜(S, Cu, Fe)、硬渣(As, Fe, Cu)、Cu—Sb 相和铅块。银在 Cu 与 Sb 形成的熔体中的溶解度比在液态铅中的高。S 与 Cu 形成冰铜,As 与 Cu 形成硬渣。S 和 As 能减少 Cu—Sb 合金的生成量,从而降低铅块中银的损失。

关键词: 铅鼓风炉; 银; 铅杂质

(Edited by Hua YANG)